

Fries: Fast and Consistent Runtime Reconfiguration in Dataflow Systems with Transactional Guarantees (Extended Version)

Zuozhi Wang, Shengquan Ni, Avinash Kumar, Chen Li
 UC Irvine
 United States
 {zuozhiw,shengqun,avinask1,chenli}@ics.uci.edu

ABSTRACT

A computing job in a big data system can take a long time to run, especially for pipelined executions on data streams. Developers often need to change the computing logic of the job such as fixing a loophole in an operator or changing the machine learning model in an operator with a cheaper model to handle a sudden increase of the data-ingestion rate. Recently many systems have started supporting runtime reconfigurations to allow this type of change on the fly without killing and restarting the execution. While the delay in reconfiguration is critical to performance, existing systems use epochs to do runtime reconfigurations, which can cause a long delay. In this paper we develop a new technique called Fries that leverages the emerging availability of fast control messages in many systems, since these messages can be sent without being blocked by data messages. We formally define consistency in runtime reconfigurations, and develop a Fries scheduler with consistency guarantees. The technique not only works for different classes of dataflows, but also works for parallel executions and supports fault tolerance. Our extensive experimental evaluation on clusters show the advantages of this technique compared to epoch-based schedulers.

PVLDB Reference Format:

Zuozhi Wang, Shengquan Ni, Avinash Kumar, Chen Li. Fries: Fast and Consistent Runtime Reconfiguration in Dataflow Systems with Transactional Guarantees (Extended Version). PVLDB, 16(2): XXX-XXX, 2022.
 doi:XX.XX/XXX.XX

PVLDB Artifact Availability:

The source code, data, and/or other artifacts have been made available at <https://github.com/Textera/Fries-Flink>.

1 INTRODUCTION

Big data systems are widely used to process large amounts of data. Each computation job in these systems can take a long time to run, from hours to days or even weeks to finish. Applications that require timely processing of input data often use pipelined dataflow execution engines [1, 9, 10, 34], for example, in the scenarios of processing real-time streaming data, or answering queries progressively to provide early results to users. In these applications, when

a long running job continuously processes ingested data, developers often need to change the computing logic of the job without disrupting the execution, as illustrated in the following example.

Consider a data-processing pipeline for payment-fraud detection shown in Figure 1. This simplified dataflow resembles many real-world applications [14, 32]. A stream of payment tuples is continuously ingested into the dataflow, with each tuple containing payment information such as customer, merchant, and amount. The dataflow uses two machine learning (ML) operators *FC* and *FM* to detect fraud based on customer and merchant information.

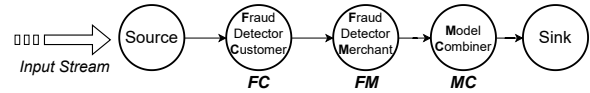


Figure 1: An example data-processing pipeline for fraud detection processing continuously ingested data.

Consider two example use cases in this dataflow. *Use case 1: fixing loopholes in operators.* After observing unexpected tuples from the Sink operator, the user identifies a loophole in the operator *FM*. She wants to update this operator to incorporate new rules to fix the loophole, without stopping the execution. *Use case 2: handling surges of data arrival rate.* Suppose the data arrival rate at the source suddenly increases, and as a result, the end-to-end processing latency becomes larger. The user finds that the ML operator *FM* is the bottleneck. To reduce the latency, she wants to “hot-replace” the expensive ML model (e.g., a deep neural network) with a light-weight model (e.g., a decision tree) to improve its performance, thus reduce the processing latency. Again, she wants to make the change without stopping the execution. These examples show the importance of allowing developers to change the dataflow execution “on the fly.” We call such changes *runtime reconfigurations*. This problem has gained a lot of interest in the research areas of software engineering [30], mobile computing [20, 33], and distributed systems [21, 23]. Recently, users of dataflow systems also show the need for runtime reconfigurations [16, 17, 32] and more systems start supporting this important feature [8], such as Amber [22], Chi [24], Flink [36], and Trisk [25].

Naturally there is a delay from the time a user requests a reconfiguration to the time its changes take effect in the target operators. This delay is critical to the performance of the system. For example, in use case 1, the user wants to fix the loophole as soon as possible since a large reconfiguration delay can cause financial losses. In use case 2, a large delay in mitigating the surge can cause the system to suffer longer in terms of long latency and wasting of computing resources. Thus we want this delay to be as low as possible.

This work is licensed under the Creative Commons BY-NC-ND 4.0 International License. Visit <https://creativecommons.org/licenses/by-nc-nd/4.0/> to view a copy of this license. For any use beyond those covered by this license, obtain permission by emailing info@vldb.org. Copyright is held by the owner/author(s). Publication rights licensed to the VLDB Endowment.
 Proceedings of the VLDB Endowment, Vol. 16, No. 2 ISSN 2150-8097.
 doi:XX.XX/XXX.XX

A main limitation of existing systems supporting runtime reconfigurations is that they could have a long reconfiguration delay. In these systems, after a reconfiguration request is submitted, they need to wait for all the in-flight tuples to be processed by those target reconfiguration operators, as well as those earlier operators in the dataflow, before the requested changes can be applied on the target operators. This delay could be very long, when there are many in-flight tuples, or some of these operators are expensive, especially for operators using advanced machine learning models and those implemented as user-defined functions (UDF’s).

In this paper, we develop a novel technique, called “Fries,” to perform runtime reconfigurations with a low delay. It leverages the emerging availability of fast control messages in many systems recently. A *fast control message*, “FCM” for short, is a message exchanged between the controller in the data engine and an operator without being blocked by data messages. Figure 2 shows an example of handling a reconfiguration request of two operators *FM* and *MC* using FCM’s. Upon a reconfiguration request, the controller sends an FCM to each of the two operators, and each of them applies the new configuration immediately after receiving the message. Since FCM’s are sent separately from data messages, these changes can reach the target operators much faster.

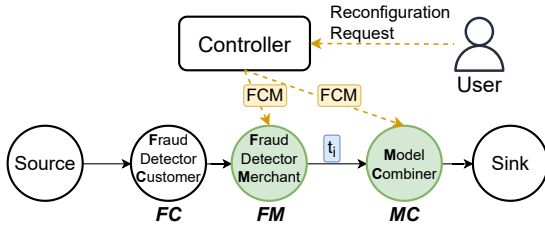


Figure 2: Handling a runtime reconfiguration of operators *FM* and *MC* using fast control messages (FCM’s).

We will show in Section 4.1 that the naive way of using FCM’s can cause consistency issues in Figure 2. It has unexpected side effects, e.g., producing incorrect results on the output tuples, or even causing the operator *MC* to crash. This example shows several challenges in developing Fries: 1) What is the meaning of “consistency” in this reconfiguration context? 2) How to ensure this consistency while reducing their delay? 3) How to deal with different types of operators and support parallel executions? We study these challenges and make the following contributions.

- We analyze epoch-based reconfiguration schedulers and show their limitations (Section 3).
- We formally define consistency of a reconfiguration based on transactions (Section 4).
- We first consider a simple class of dataflows that have one-to-one operators only, and develop a Fries scheduler that guarantees consistency (Section 5).
- We then consider the general class of dataflows with one-to-many operators, and extend the Fries scheduler (Section 6).
- We extend Fries to more general cases, such as dataflows with blocking operators and multiple workers. We also discuss how to support fault-tolerance (Section 7).

- We conduct an extensive experimental study to evaluate Fries in various scenarios and show its superiority compared to epoch-based schedulers (Section 8).

1.1 Related Work

Reconfiguration systems. Recently, many data-processing systems have started to support reconfigurations. Flink [9] supports reconfiguration by taking a savepoint [15], killing the running job, then restarting the job with the new configuration. This approach is disruptive to the dataflow execution. Spark Streaming [2, 39] uses a mini-batch-based execution strategy and supports reconfiguration between mini-batches. Chi [24] enables runtime reconfiguration by propagating epoch markers in its data stream. Trisk [25] provides an easy-to-use programming API for reconfigurations. The approaches in these systems are all based on epochs, which can have a long reconfiguration delay, as analyzed in Section 3. Fries relies on FCM’s to perform reconfigurations with a low delay. Noria [18] is a system that uses dataflows to incrementally maintain materialized views. The system supports reconfigurations of view definitions, which require the new views to be recomputed from entire base tables. In Fries, an update of a dataflow only affects the future tuples. The input tuples that are already processed by the dataflow are not recomputed using the new configuration.

Re-scaling systems. Some systems [13, 19, 27] support updating the dataflow for re-scaling. For example, Megaphone [19] based on timely dataflow [28] supports a fine-granularity re-scaling and Rhino [27] based on Flink supports re-scaling with very large states. Fries focuses on reconfiguring the computation functions of operators, which is different from re-scaling.

Transactions in dataflow systems. S-Store [26] and the work in [5] are systems that allow streaming dataflows and OLTP workloads to access a shared mutable state. Although both systems do not support reconfigurations directly, we could map a reconfiguration to these systems. S-Store defines transactions on the processing of each input batch on a single operator. This model cannot express our consistency requirements in reconfigurations. The work in [5] treats a dataflow as a black box, thus it has the limitation of not being able to utilize the properties of the dataflow and its operators to reduce the reconfiguration delay. Fries can do so to achieve this reduction. Both earlier systems include a transaction scheduler to manage the processing of data, which creates scheduling overhead even when there is no reconfiguration. The Fries scheduler has no such overhead before receiving a reconfiguration request. Additionally, both earlier systems are only on a single node, while the Fries scheduler can run on a distributed engine on a cluster.

Transactions in database systems. Transactions are widely studied in traditional database systems (e.g., [3, 4, 37]). A uniqueness in transactions in our work is that they treat operations in a reconfiguration as a separate transaction, which is handled differently from data transactions. In addition, Fries does optimizations by utilizing special properties in our problem setting, including the DAG shape of a dataflow, and types of operators, e.g., one-to-one and one-to-many. Moreover, the Fries scheduler uses FCM’s and epoch markers to schedule transactions without locking.

2 PROBLEM SETTINGS

2.1 Data-Processing Model

A data-processing system runs a computation dataflow job represented as a directed acyclic graph (DAG) of operators. Each operator receives tuples from its input edges, processes them, and sends tuples through its output edges. An operator contains a computation function f represented as

$$f : (s, t) \rightarrow (s', \{(t'_1, o'_1), \dots, (t'_n, o'_n)\}).$$

The function processes a tuple t at a time with a state s of the operator, produces a set of zero or more output tuples $\{t'_1, \dots, t'_n\}$, where each tuple t'_i has a receiving operator o'_i . The operator also updates its state to s' . The system has a module called *controller* that manages the execution of the job, handles requests from the user, and exchanges messages with operators during the execution.

For simplicity, we first focus on dataflows under the following assumptions. (1) A dataflow contains pipelined operators only, such as selection, projection, union, and other tuple-at-a-time operators. We consider a class of join operators where the operator first collects all the tuples from one input (e.g., the “build” input of a hash join), then starts processing tuples from the other input (e.g., the “probe” phase of a hash join). We consider the processing of tuples from the second input of join. (2) Each operator has a single worker. We relax these assumptions in Section 7.

As an example, consider a data-processing pipeline for payment-fraud detection shown in Figure 1. The example dataflow uses two machine learning (ML) operators for fraud detection. The first one, denoted as *FC*, keeps a state of the 5 recent tuples of each customer. For each input tuple, *FC* updates the state and feeds the 5 recent tuples of the customer into an ML model. The predicted probability $p_c(5)$ is attached as a new column of the tuple. The second one, denoted as *FM*, keeps a state of the 5 recent tuples of each merchant. Similarly, it uses an ML model to generate a predicted probability $p_m(5)$, and attaches it as a new column of the tuple. Finally, the model combiner *MC* uses $p_c(5)$ and $p_m(5)$ of each tuple to compute the final average probability with the weights $[0.4, 0.6]$.

2.2 Runtime Reconfiguration

Definition 2.1 (Runtime reconfiguration). During the execution of a dataflow, an update to the computation functions of its operators is a *runtime reconfiguration* of this execution.

Formally, a reconfiguration \mathcal{R} is a set of operators with a function update $\mu(o_i)$ for each operator o_i , i.e.,

$$\mathcal{R} = \{(o_1, \mu(o_1)), \dots, (o_n, \mu(o_n))\}.$$

Each operator o_i has a *function-update operation* $\mu(o_i)$. This operation applies a pair $\langle f'_{o_i}, \mathcal{T}_{o_i} \rangle$ to the operator, where f'_{o_i} is a new computation function of the operator. \mathcal{T}_{o_i} is a state transformation that converts the operator’s original state s to a new state $s^* = \mathcal{T}_{o_i}(s)$, which can be consumed by f'_{o_i} . In this paper, we consider the case where there is one reconfiguration at a time.

In the running example, suppose the user identifies a flaw in the dataflow and wants to reconfigure the two operators *FM* and *MC*. Specifically, the user wants to change *FM* to output an additional probability value $p_m(10)$, which is predicted using the 10

recent tuples of each merchant. The operator *MC* needs to be updated to combine all three probabilities ($p_c(5)$, $p_m(10)$, and $p_m(5)$) with the new weights $[0.4, 0.4, 0.2]$. Table 1 shows the old and new configurations of the two reconfiguration operators.

	<i>FM</i> ’s output	<i>MC</i> weights
Old configuration	$p_m(5)$	$[0.4, 0.6]$
New configuration	$p_m(10), p_m(5)$	$[0.4, 0.4, 0.2]$

Table 1: Operator executions during a reconfiguration.

Note that the new configuration of an operator can require a state different from that of the old configuration. In this case, the reconfiguration can use a state transformation to migrate the old state to the new one. In the running example, the old configuration of operator *FM* uses a state with the last 5 payment tuples for each merchant. However, the new configuration of *FM* needs a list of last 10 tuples for each merchant. The user provides a state transformation \mathcal{T} for operator *FM*, to instruct the system in transferring operator *FM*’s old state to the new one. In this example, the user chooses to fill the new state with the 5 tuples from the old state and 5 additional *null* values.

3 EPOCH-BASED RECONFIGURATION SCHEDULERS AND LIMITATIONS

In this section, we explain epoch-based reconfiguration schedulers and show their limitation of long delays.

3.1 Epoch-Based Schedulers

Dataflow epoch. A stream of tuples processed by the system can be divided into consecutive sets of tuples, where each set is called an *epoch* [6]. One way to create epochs is to use epoch markers. At the start of a new epoch, an epoch marker is injected to each source operator. The epoch marker is then propagated along the data stream using the following protocol [6]. When an operator receives an epoch marker from an input channel, it performs epoch alignment by waiting for all its inputs to receive an epoch marker, then sends the marker downstream. As an example, Figure 3 shows two epochs during the execution of the fraud-detection dataflow. An epoch marker injected between t_4 and t_5 divides the input stream into two epochs. The epoch marker indicates the end of epoch 1 and the start of epoch 2.

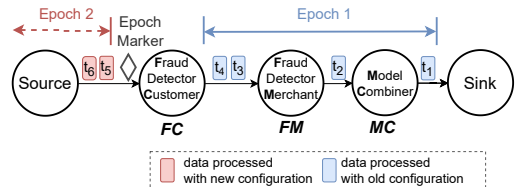


Figure 3: An epoch-based reconfiguration scheduler in Chi [24]. It uses an epoch barrier to apply the new configuration to operators *FM* and *MC* at the start of Epoch 2.

Definition 3.1 (Epoch-based Scheduler). An epoch-based scheduler schedules a reconfiguration request between two epochs. That is, for each reconfiguration operator O , all the tuples in the old epoch are processed with the old configuration of O , and all the tuples in the new epoch are processed with the new configuration of O .

Considering the aforementioned method to generate epochs, the following is an implementation adopted by Chi [24]. We call this implementation “Epoch Barrier Reconfiguration” scheduler, or “EBR” in short. Upon a reconfiguration request, the controller starts a new epoch and piggybacks the reconfiguration in the epoch marker. When a reconfiguration operator receives epoch markers from all its inputs, it applies the new configuration. The operator then processes the input tuples in the next epoch using the new configuration. Figure 3 shows the process of handling a reconfiguration of operators FM and MC using the EBR scheduler. When operator FM receives the epoch marker, it applies the new configuration, and propagates the marker to operator MC . When operator MC receives the epoch marker, it also applies the new configuration.

System	Epoch creation	Reconfiguration Strategy
Chi [24]	Epoch makers	Piggybacking control messages in epoch markers
Flink [15]	Epoch makers	Stop-and-restart
Spark Streaming [2]	Mini-batch	Stop-and-restart

Table 2: Epoch-based reconfiguration schedulers.

Table 2 shows different epoch-based reconfiguration schedulers.

In Flink [15], upon a reconfiguration, a new epoch is immediately triggered using an epoch marker. At the end of the old epoch, each operator saves its state into a checkpoint. After the old epoch is processed by all the operators, Flink kills the execution, updates the dataflow graph, loads the saved states, and restarts the dataflow. In Spark Streaming [2], epochs are created by dividing the input data stream into small mini-batches, each of which is an epoch. A mini-batch is processed one at a time by launching a separate computation job. Upon a reconfiguration, the system modifies the dataflow graph before starting the job of the next mini-batch.

3.2 Limitations: Long Reconfiguration Delays

A major limitation of epoch-based reconfiguration schedulers is a long reconfiguration delay, which is from the time a request is submitted to the time the new configuration takes effect in the target operators. In particular, the system needs to process all the in-flight tuples before the new epoch. Take the EBR scheduler in Figure 3 as an example. Operator FM needs to finish processing the in-flight tuples t_3 and t_4 . In general, this delay could be long due to the following reasons. First, the dataflow can contain multiple expensive operators that make the processing of an epoch slow. Second, the number of in-flight tuples could be large, especially when the system is under high workload. We may want to reduce the number of in-flight tuples by decreasing the buffer size. However, a smaller buffer can be easily filled by a minor fluctuation in the input ingestion rate. When the buffer is full, the system triggers back-pressure, which can decrease the throughput. Moreover, a small buffer size causes the networking layer to transmit data in

small batches, which introduces additional transmission overhead. Compared to the EBR approach, the Flink approach suffers from an additional delay of stopping and restarting the dataflow. Spark Streaming can also have a long reconfiguration delay. The delay is determined by the processing time of a mini-batch, with a predefined interval usually set to a few seconds. However, the delay can be higher when the processing speed cannot keep up with a surge of the data ingestion rate.

4 SCHEDULING RECONFIGURATIONS USING FAST CONTROL MESSAGES

In this section, we introduce a new type of reconfiguration schedulers based on fast control messages (FCM’s). We present a naive scheduler and show its issues. We then formally define consistency of a reconfiguration.

Definition 4.1 (Fast Control Message). A fast control message, “FCM” for short, is a message exchanged between the controller and an operator without being blocked by data messages.

There are many ways to implement fast control messages. For instance, to send an FCM from the controller to the fraud detector in our running example, one approach is to set up a new communication channel between the controller and the fraud detector. The channel is separate from existing data channels, and the FCM can bypass data messages. Another way is to transmit the FCM using existing data channels, but assigning a higher priority to the FCM. The FCM is first sent to a source operator of the workflow, then propagated along the edges to the fraud detector, and it bypasses data messages in each data channel.

4.1 FCM-based Schedulers

Naive FCM scheduler. A main benefit of using FCM’s to schedule reconfigurations compared to epoch-based schedulers is that FCM’s have a much smaller delay. A naive scheduler leverages this benefit as follows. The controller sends an FCM directly to each reconfiguration operator. When an operator receives an FCM, it applies the new configuration immediately after finishing the processing of its current tuple. We use Figure 2 to explain how the naive scheduler works in a reconfiguration of two operators FM and MC . Using this scheduler, the controller sends an FCM directly to each of the two operators FM and MC . The FCM carries the new function f' and the state transformation \mathcal{T} of the corresponding operator. These operators update their configuration after receiving their FCM.

While this naive scheduler has a low reconfiguration delay, it could generate an undesirable reconfiguration schedule in this example. Notice that the scheduler does not coordinate the updates to these two operators that run independently. Consider the in-flight tuple t_i , which is processed by FM using its old configuration. Suppose the MC switches to the new configuration before the arrival of t_i . Then tuple t_i is processed by MC using its new configuration. The tuple contains two probability values $p_c(5)$ and $p_m(5)$, but the new configuration of MC expects three probability values. This schema mismatch could have unexpected side effects, such as an incorrect result on the produced output tuple, or even causing the operator MC to crash. This example shows the importance for the reconfiguration to be performed in a synchronized manner on the

two reconfiguration operators. In particular, we want a tuple to be processed by the two operators either using the old configuration or using the new configuration.

FCM multi-version scheduler. To ensure a tuple is processed by the same configuration of multiple operators, we can use the following FCM-based multi-version scheduler that maintains multiple configurations of an operator at the same time. The controller first sends an FCM to each reconfiguration operator. Each operator keeps both the old configuration and the new one. After all operators have received the FCM, each source operator increments its version number, which is tagged to each source tuple. For each input tuple, an operator checks the tuple’s tagged version number, chooses the corresponding configuration version to process the tuple, and tags the same version number to the output tuples. As an example, in Figure 4, after the new configuration is sent to operator E , the source operators then tag subsequent output tuples t_3 and t_4 with the new version v_2 .

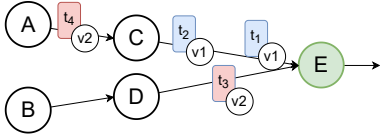


Figure 4: Using an FCM multi-version scheduler, an operator processes a tuple based on its version tag.

This scheduler has two problems. First, each reconfigured operator may need to keep two sets of states for two configurations, and these states could be very large (e.g., large hash tables or machine learning models). Second, this scheduler still suffers from a possible high reconfiguration delay. In particular, similar to the case of the EBR scheduler, there can be a large amount of in-flight tuples that are already tagged with the old version and they still need to be processed with the old configuration (e.g., t_1 and t_2 in Figure 4).

4.2 Reconfiguration Consistency

We formally define the consistency requirements in this context. At a high level, we treat the processing of a single source tuple by multiple operators as one *transaction*, and a reconfiguration as another transaction. We use conflict-serializability to define the consistency of a schedule of a reconfiguration.

Definition 4.2 (Scope of a source tuple). The *scope* of a source tuple t of a dataflow W , denoted as $\mathcal{S}(W, t)$, is a pair $(\mathcal{S}, \leq_{\mathcal{S}})$, where \mathcal{S} is a set of tuples and $\leq_{\mathcal{S}}$ is a partial order on \mathcal{S} , defined as follows:

- (1) The source tuple is in \mathcal{S} .
- (2) For each tuple s in \mathcal{S} , if an operator processes the tuple s and produces zero or more output tuples $\{s'_1, \dots, s'_n\}$, all the produced tuples are also in \mathcal{S} . For each tuple s'_i , we have the order $s < s'_i$ in $\leq_{\mathcal{S}}$.

For instance, in Figure 5, a source tuple t is ingested into the dataflow from the source operator A and processed by operators C , D , E , F , and H . The scope of t includes the tuples on the highlighted edges and their partial order defined as their edges on the DAG.

Definition 4.3 (Data operation). The *data operation* of a tuple s is the processing of s by its receiving operator o , denoted as $\phi(s, o)$.

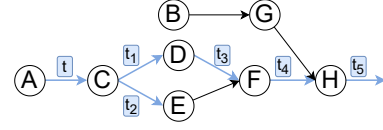


Figure 5: Scope of a source tuple in a dataflow.

Definition 4.4 (Data transaction). For a dataflow W and a source tuple t in W , let $(\mathcal{S}, \leq_{\mathcal{S}})$ be the scope of t . The *data transaction* of t is a pair (Φ, \leq_{Φ}) , where Φ is the set of data operations of the tuples in \mathcal{S} , and \leq_{Φ} is a partial order on Φ . For two data operations $\phi(t_i, o_i)$ and $\phi(t_j, o_j)$ in Φ , we have $\phi(t_i, o_i) < \phi(t_j, o_j)$ in \leq_{Φ} if and only if $t_i < t_j$ is in $\leq_{\mathcal{S}}$.

For instance, in Figure 2, tuple t has the following data transaction T_1 :

$$T_1 : [\phi(t, FC), \phi(t, FM), \phi(t, MC)].$$

In the data transaction, “ $\phi(t, FC)$ ” is a data operation representing the processing of this tuple t by the FC operator.

Definition 4.5 (Function-update transaction). The *function-update transaction* of a reconfiguration $\mathcal{R} = \{(o_1, \mu(o_1)), \dots, (o_n, \mu(o_n))\}$ on a dataflow W is the set $\{\mu(o_1), \dots, \mu(o_n)\}$, where each $\mu(o_i)$ is a function-update operation in \mathcal{R} .

For instance, the reconfiguration in Figure 2 has the following function-update transaction T_2 :

$$T_2 : \{\mu(FM), \mu(MC)\}.$$

In the function-update transaction, “ $\mu(FM)$ ” is a function-update operation representing that the operator FM switches to the new configuration. Note that the order of different operations in a function-update transaction does not matter because they update different operators and are independent of each other.

Definition 4.6 (Conflicting operations). A data operation $\phi(t, o)$ and a function-update operation $\mu(o')$ are said to be *conflicting* if $o = o'$, i.e., they are on the same operator. They are said to be *not conflicting* if $o \neq o'$.

For instance, in Figure 2, operations $\phi(t, FM)$ and $\mu(FM)$ are conflicting because they are on the same operator. Operations $\phi(t, FC)$ and $\mu(FM)$ are not conflicting as they are on different operators.

Definition 4.7 (Schedule). A *schedule* of a set of transactions T_1, \dots, T_k is the set of all the operations in those transactions with a *partial order*. The schedule is called *serial* if for each pair of transactions T_i and T_j , T_i ’s operations in the schedule are either all before those in T_j or all after those in T_j .

In this paper we only consider schedules that include one function-update transaction and many data transactions.

Definition 4.8 (Conflict-equivalence). Two schedules S_1 and S_2 of the same set of transactions are said to be *conflict-equivalent* if $\forall o_i, o_j \in S_1$, if o_i and o_j are conflicting, and o_i is before o_j in S_1 , then o_i is also before o_j in S_2 .

Definition 4.9 (Conflict-serializable). A schedule is said to be *conflict-serializable* if it is conflict-equivalent to a serial schedule of the same set of transactions.

In the rest of the paper, when a partial order of a data transaction or a schedule defines a total order, for simplicity, we just show the transaction or the schedule as a sequence. We use the running example in Figure 1 to explain these concepts.

- S_1 is a schedule of the two transactions T_1 and T_2 :

$$S_1 : [\phi(t, FC), \mu(FM), \phi(t, FM), \mu(MC), \phi(t, MC)].$$

- S_2 is a serial schedule of the two transactions:

$$S_2 : [\mu(FM), \mu(MC), \phi(t, FC), \phi(t, FM), \phi(t, MC)].$$

In particular, all T_2 's operations in this schedule are before those in T_1 .

- S_1 and S_2 are conflict-equivalent. For example, for the conflicting pair $\mu(FM)$ and $\phi(t, FM)$, the former is before the latter in both schedules.
- S_1 is conflict-serializable because it is conflict-equivalent to the serial schedule S_2 .
- S_3 is not a conflict-serializable schedule:

$$S_3 : [\phi(t, FC), \phi(t, FM), \mu(FM), \mu(MC), \phi(t, MC)].$$

We can show that S_3 is not conflict-equivalent to any serial schedule. Intuitively, it has two pairs of conflicting operations, namely $[\phi(t, FM), \mu(FM)]$ and $[\mu(MC), \phi(t, MC)]$, and their corresponding transaction orders are different.

S_3 is the “bad” schedule generated by the naive FCM scheduler in Section 4.1, in which tuple t is processed using the old configuration of FM and the new configuration of MC . Schedule S_1 is a “good” schedule since t is processed entirely using the new configurations of both operators FM and MC and the aforementioned schema-mismatch issue does not happen.

Consistency of epoch-based schedulers. Consider the example in Figure 1. The aforementioned schedule S_1 in Section 4.2 is produced by the EBR epoch-based scheduler, where the epoch marker is propagated before tuple t . We show that the EBR approach can always produce a conflict-serializable schedule in Lemma 4.10. We also show that in general, an epoch-based scheduler always produces conflict-serializable schedules in Lemma 4.11.

LEMMA 4.10. *Every schedule produced by the EBR epoch-based scheduler is conflict-serializable.*

PROOF. Let S be a produced schedule. We construct a serial schedule S' using the following steps. Consider the function-update transaction U and each data transaction T for a tuple t . Since the epoch marker serve as a barrier dividing the input stream into two epochs, t can be in only one of the following two cases:

- t is before the epoch marker. For each conflict in S between a data operation ϕ in T and a function-update operation μ in U , ϕ is before μ . We place T before U in S' . Thus, in S' , ϕ is also before μ .
- t is after the epoch marker. Similarly, we place T after U in S' . Each conflict order in S remains the same in S' .

For those data transactions before U , we order them in S' following the order of their first data operations in S . For data transactions after U , we order them in S' following the order of their first data operations in S . Notice that there are no conflicts between two data transactions.

The schedule S is conflict-equivalent to the constructed serial schedule S' because all conflicting pairs in S have the same order in S' . Therefore, S is conflict-serializable. \square

LEMMA 4.11. *Every schedule produced by a general epoch-based scheduler is conflict-serializable.*

PROOF. Consider a function-update transaction U and each data transaction T for a source tuple t . For a general epoch-based scheduler, all the tuples in the scope of t are in one epoch E_t and U is scheduled between two epochs E_i and E_{i+1} . We can compare E_t with the boundary between E_i and E_{i+1} to determine the position of T in a serial schedule. We can prove this claim using steps similar to those in the proof of Lemma 4.10. \square

5 DATAFLOWS WITH ONE-TO-ONE OPERATORS ONLY

In this section, we consider the case where a dataflow contains one-to-one operators only. We propose a scheduler called Fries, which uses FCM's to achieve low reconfiguration delay and still guarantees conflict-serializability of produced schedules.

Definition 5.1 (One-to-one operator). An operator is called *one-to-one* if its processing function emits at most one (tuple, receiving operator) pair for each input tuple.

This type includes operators such as projection, filter, map function, equi-join on key attributes, and union.

Definition 5.2 (One-to-many operator). An operator is called *one-to-many* if its processing function can emit more than one output (tuple, receiving operator) pair for an input tuple.

This type includes operators such as join on non-key attributes and flatten function. In the rest of this section, we consider dataflows where all operators in the dataflow are one-to-one.

5.1 Conflict-Serializable Schedules Produced by the Naive FCM-based Scheduler

Section 4.1 shows an example dataflow and a reconfiguration where the naive FCM-based scheduler produces a non-conflict-serializable schedule. Next we use an example to show that the naive scheduler can still guarantee conflict-serializability for some types of dataflows and reconfigurations.

Example 5.3. Suppose we want to use the naive FCM-based scheduler to handle a reconfiguration of the two operators C and D as shown in Figure 6. Operator X is a one-to-one operator that splits the outputs tuples to operators C and D . In this case, we have a data transaction $T_3 = [\phi(t_1, X), \phi(t_1, C)]$, another data transaction $T_4 = [\phi(t_2, X), \phi(t_2, D)]$, and a function-update transaction $U = [\mu(C), \mu(D)]$. The controller sends two separate FCM's to C and D . Consider a possible schedule with T_3 , T_4 , and U :

$$S_4 : [\phi(t_1, X), \mu(C), \phi(t_1, C), \phi(t_2, X), \mu(D), \phi(t_2, D)].$$

Schedule S_4 is conflict-serializable because it is conflict-equivalent to the serial schedule $[U, T_3, T_4]$. Interestingly, we can show that all schedules produced by the naive FCM-based scheduler in Figure 6 are conflict-serializable.

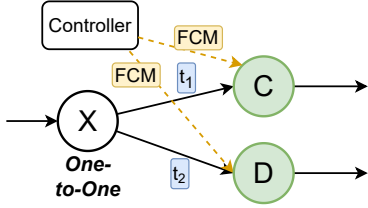


Figure 6: An example dataflow with a reconfiguration on operators C and D . The naive FCM-based scheduler always produces a conflict-serializable schedule.

One might wonder why the two examples in Figure 2 and Figure 6 are different in the conflict-serializability of the produced schedules. The main reason is that in Figure 2, a tuple can be processed by operators FM and MC , and both of them are in the reconfiguration. But there is no synchronization between the data operations and the function-update operations, causing the non-conflict-serializability. While in Figure 6, a tuple is processed by only one of the two paths through either C or D . On each path, there is a single operator in the reconfiguration, thus the data operations and the function-update operations are always synchronized.

Next, we introduce a concept called “minimal covering sub-DAG,” which is used to represent the synchronization components. We then describe the Fries scheduler using this concept, and prove that this scheduler can always produce a conflict-serializable schedule.

5.2 Minimal Covering Sub-DAG (MCS)

Definition 5.4 (Minimal covering sub-DAG). Given a DAG $G = (V, E)$, and a set of vertices $M \subseteq V$, a minimal covering sub-DAG $G' = (V', E')$ is defined as follows:

- (1) $M \subseteq V'$;
- (2) $\forall A, B \in M$, if there is a path from A to B , then all the vertices and edges on the path are in V' and E' , respectively;
- (3) G' is minimal, i.e., no proper sub-DAG of G' can satisfy the above two conditions.

LEMMA 5.5. *There is a unique MCS given a DAG and a set of vertices.*

PROOF. Suppose G'_1 and G'_2 are two distinct MCS's of a DAG and a set of vertices M . Consider the sub-DAG G'_3 that is the “intersection” of G'_1 and G'_2 , i.e., the vertices of G'_3 are the intersection of the two sets of vertices in G'_1 and G'_2 , the edges of G'_3 are the intersection of the two sets of edges in G'_1 and G'_2 . Since M is a subset of the sets of vertices in G'_1 and G'_2 , M is also a subset of the vertices in G'_3 . Thus G'_3 satisfies property (1). $\forall A, B \in M$, if there is a path p from A to B , p is also in both G'_1 and G'_2 , so p is also in the G'_3 . Thus G'_3 also satisfies property (2). Therefore, G'_3 is also an MCS, which contradicts the minimality property (3) of G'_1 and G'_2 . \square

Algorithm 1 shows an algorithm for finding the minimal covering sub-DAG (MCS) given a DAG G and a set of vertices M . In lines 5- 10, we iterate through the DAG in a topological order. For each vertex v , we mark v in “red” if v is in M or any parent vertex of v is marked in “red.” After this iteration, a vertex marked in “red” is either 1)

in M , or 2) a descendant of a vertex in M . Next in lines 11- 16, we iterate through the DAG in a reverse topological order. For each vertex v , we mark v in “blue” if v is in M or any child of v is marked in “blue.” After this iteration, a vertex marked in “blue” is either 1) in M , or 2) is an ancestor of a vertex in M . Finally, in lines 18- 20, we add all the vertices marked in both “red” and “blue” to the MCS because these vertices are either 1) in M , or 2) on a path between two operators in M . Then we add all the edges connecting these vertices to the MCS.

The time complexity of this algorithm is $O(V + E)$, specifically:

- The topological ordering in line 4 takes $O(V + E)$ [11];
- The loop of marking “red” in lines 5- 10 takes $O(V + E)$ because we iterate through each vertex once and look at every edge once;
- Similarly, the loop of marking “blue” in lines 11- 16 also takes $O(V + E)$;
- The loop in lines lines 18- 20 takes $O(V)$ and the loop in lines lines 22- 24 takes $O(E)$.

Algorithm 1 Find Minimal Covering SubDAG

Input: dataflow DAG $G = (V, E)$

Input: $M = \{m_1, \dots, m_n\}$

```

1:  $D \leftarrow \emptyset$ 
2: for each  $v \in V$  do
3:    $D[v] \leftarrow \emptyset$ 
4: let  $v_1, \dots, v_{|V|}$  be a topological ordering of  $G$ 
5: for each  $v \leftarrow v_1, \dots, v_{|V|}$  do
6:   if  $v \in M$  then
7:     add “red” to  $D[v]$ 
8:   for each incoming edge  $e$  of  $v$  do
9:     if “red”  $\in D[e.from]$  then
10:      add “red” to  $D[v]$ 
11: for each  $v \leftarrow v_{|V|}, \dots, v_1$  do
12:   if  $v \in M$  then
13:     add “blue” to  $D[v]$ 
14:   for each outgoing edge  $e$  of  $v$  do
15:     if “blue”  $\in D[e.to]$  then
16:       add “blue” to  $D[v]$ 
17:  $V' = \{\}$ 
18: for each  $v \in V$  do
19:   if  $D[v] = \{\text{“red”}, \text{“blue”}\}$  then
20:     add  $v$  to  $V'$ 
21:  $E' = \{\}$ 
22: for each  $e \in E$  do
23:   if  $e.from \in V' \wedge e.to \in V'$  then
24:     add  $e$  to  $E'$ 
25: return  $(V', E')$ 

```

Figure 7 shows the minimal covering sub-DAG for the dataflow graph in Figure 5 and the set of operators $\{C, F, G\}$ in the reconfiguration. The sub-DAG is: $V' = \{C, D, E, F, G\}$ and $E' = \{C \rightarrow D, C \rightarrow E, D \rightarrow F, E \rightarrow F\}$. In general, we can show that there is a unique MCS given a DAG and a set of vertices, and we can compute the MCS using an algorithm with an $O(V + E)$ time complexity.

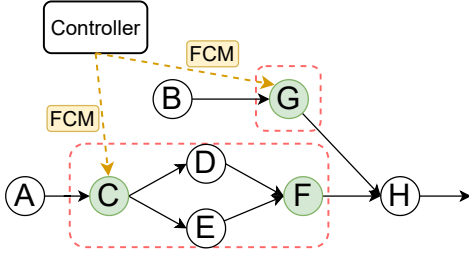


Figure 7: Two components of the minimal covering sub-DAG used in the Fries scheduler are highlighted in red.

5.3 The Fries Scheduler

The Fries scheduler uses components of the MCS to schedule the reconfiguration. A *component* is a maximal sub-DAG of the MCS where every pair of vertices in the component are connected by a path, ignoring the direction of edges. For example, the sub-DAG in Figure 7 has two components, each marked in a red box. The components of the MCS can be also computed using an algorithm [12] with an $O(V + E)$ time complexity.

The Fries scheduler is formally described in Algorithm 2. We first construct the minimal covering sub-DAG from the original dataflow DAG and operators in the reconfiguration (lines 1 and 2). We compute the components within the MCS (line 3). For each component in the MCS, the controller sends an FCM to the “head” operators, i.e., those with no input edges in the component. The head operators then start propagating an epoch marker within the component (lines 4 to 6). Specifically, when an operator receives an epoch marker, it performs marker alignment on the input edges in its component. An operator sends an epoch marker only to its downstream operators in its component.

Algorithm 2 The Fries Scheduler (for dataflows with one-to-one operators only)

Input: $G = (V, E)$
Input: $\mathcal{R} = \{(o_1, U_1), \dots, (o_n, U_n)\}$

- 1: $M \leftarrow \{o_1, \dots, o_n\}$
- 2: $G' \leftarrow \text{findMCS}(G, M)$
- 3: $C_1, \dots, C_p \leftarrow \text{findComponents}(G')$
- 4: **for** each $C \leftarrow C_1, \dots, C_p$ **do**
- 5: send an FCM to the each head operator in C
- 6: start propagating an epoch marker within C

As an example, in Figure 7, the controller sends an FCM to operator C , which is the only head operator of the first component. The controller also sends an FCM to operator G , which is the only head operator of the second component. When C receives the FCM, it applies the new configuration and starts propagating an epoch marker to operators D and E . These operators then forward the marker to operator F . When F receives the marker from both D and E , it applies the new configuration and stops the marker propagation. When operator G receives the marker, it applies the new configuration and does not send out an epoch marker.

Next, we show that the Fries scheduler can always produce a conflict-serializable schedule.

LEMMA 5.6. Consider a dataflow graph G with one-to-one operators only, with a reconfiguration \mathcal{R} , and the MCS G' generated by Algorithm 2. Each component of G' contains at least one reconfiguration operator.

PROOF. By the construction of Algorithm 2, the set of reconfiguration operators M in \mathcal{R} are used to construct the MCS G' . Suppose all the vertices in a component C of G' are not in M . We construct a new DAG G'' by removing all the vertices and edges in C from G' . Using similar steps as in Lemma 5.5, we can show that G'' is still a minimal covering sub-DAG of G and M . This result contradicts the minimality property of G' . \square

LEMMA 5.7. In dataflows with one-to-one operators only, consider a dataflow graph G with a reconfiguration \mathcal{R} , and the MCS G' generated by Algorithm 2. For each source tuple, the operators in its data transaction overlap with at most one component of G' .

PROOF. Suppose the operators processing a tuple t overlap with two components C_1 and C_2 in the MCS. Based on Lemma 5.6, there is an operator A in C_1 and another operator B in C_2 , where $A, B \in M$. In dataflows with one-to-one operators only, tuple t goes through a *chain* of operators and there must be a path between A and B in G . By Definition 5.4, the path must also be in G' . By the definition of components, A and B must be in the same component of G' , which contradicts the assumption. \square

THEOREM 5.8. In dataflows with one-to-one operators only, the Fries scheduler in Algorithm 2 always produces a conflict-serializable schedule.

PROOF. Let S be a produced schedule. We can construct a serial schedule S' using the following steps. Consider the function-update transaction U and each data transaction T for a tuple t . Based on Lemma 5.7, T can be in only one of the following two cases. (1) Operators in T do not overlap with any component in the MCS. In this case, T does not have any conflict with U . We can place T before U in S' . (2) Operators in T overlap with one component in the MCS. In this case, we place T in S' by comparing the position of a tuple and the epoch marker of this component. In both cases, for those data transactions before U , we order them in S' following the order of their first data operations in S . For data transactions after U , we order them in S' following the order of their first data operations in S . Notice that there are no conflicts between two data transactions. The schedule S is conflict-equivalent to the constructed serial schedule S' because all conflicting pairs in S have the same order in S' . Therefore, S is conflict-serializable. \square

The reconfiguration delay of the Fries scheduler is decided by the size of each MCS component, which is the number of edges in the component. Compared to the EBR scheduler, the FCMs sent to the head of each MCS component are not blocked by the processing of data by the upstream operators. Within each MCS component, the Fries scheduler still relies on epoch markers. In the extreme case where the MCS covers the entire dataflow graph, the Fries scheduler essentially becomes the epoch-based scheduler, where the FCMs are sent to all source operators and the epoch markers need to be propagated through the entire dataflow.

6 DATAFLOWS WITH ONE-TO-MANY OPERATORS

In this section we consider dataflows with one-to-many operators.

6.1 Challenges

Figure 8 shows a part of a dataflow with a one-to-many Join operator, which joins each input tuple with the Merchants table. When a tuple contains purchases from multiple merchants, Join generates multiple output tuples. For instance, the tuple t_1 joins with three merchants and produces the tuples t_2 , t_3 , and t_4 . The Split operator splits the stream based on merchant information and sends different tuples to the two merchant fraud-detector operators FMX and FMY . The prediction results are combined by a Union operator.

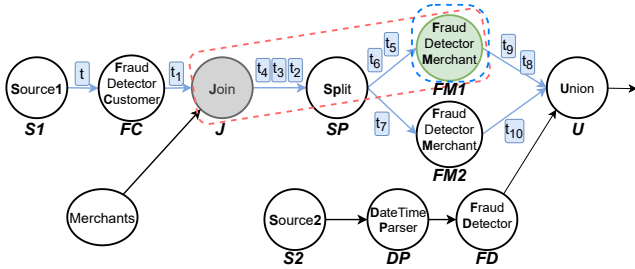


Figure 8: Reconfiguration of operator $FM1$ in a dataflow with a one-to-many Join operator. An incorrect MCS generated by Algorithm 2 is highlighted in blue. The correct MCS generated by Algorithm 3 is highlighted in red.

Based on Definition 4.4, the source tuple t has the following data transaction T_5 .

$$\Phi \text{ in } T_5 : \{\phi(FC, t), \phi(J, t_1), \phi(SP, t_2), \phi(SP, t_3), \phi(SP, t_4), \phi(FMX, t_5), \phi(FMX, t_6), \phi(FMY, t_7), \phi(U, t_8), \phi(U, t_9), \phi(U, t_{10})\}.$$

We use an example to show that when reconfiguring a dataflow with one-to-many operators, a naive adoption of the Fries scheduler in Algorithm 2 can produce a non-conflict-serializable schedule. Consider a reconfiguration of operator FMX in Figure 8. Algorithm 2 adds the only reconfiguration operator FMX to the set M and computes the MCS with one component, which contains the operator FMX and no other edges. Algorithm 2 ignores the Join operator because it is not in the reconfiguration. The method sends an FCM to FMX . This operator does not propagate the FCM to its downstream operators because it is the only operator in the MCS component. Suppose the FCM sent to operator FMX arrives *after* the tuple t_5 and *before* the tuple t_6 in the same transaction. Then this scheduler produces the following schedule with a total order of the data operations and the function-update operations:

$$S_5 : [\phi(FC, t), \phi(J, t_1), \phi(SP, t_2), \phi(SP, t_3), \phi(SP, t_4), \phi(FMX, t_5), \phi(FD_1), \phi(FMX, t_6), \phi(FMY, t_7), \phi(U, t_8), \phi(U, t_9), \phi(U, t_{10})].$$

We can show that the schedule S_5 is not conflict-serializable. Intuitively, as indicated in the operations in bold, tuple t_5 is processed by FMX with the old configuration, and tuple t_6 in the same transaction is processed by FD_2 with the new configuration.

6.2 Extending the Fries scheduler

We extend the Fries scheduler Algorithm 2 to produce a conflict-serializable schedule for a dataflow with one-to-many operators and a function-update transaction. Intuitively, for a one-to-many operator, each of its descendant operators could receive multiple input tuples that belong to the same data transaction. In Figure 8, operator SP receives three tuples (t_2 , t_3 , and t_4), and operator FMX receives two tuples (t_5 and t_6) in the same data transaction.

Consider a reconfiguration that includes the operator FD_1 . The function-update operation $\mu(FD_1)$ can be conflicting with the data operations of tuples t_5 and t_6 (in the same data transaction) in the same operator. To guarantee a conflict-serializable schedule, these two data operations must synchronize with $\mu(FMX)$ to ensure that both data operations are either before $\mu(FMX)$ or after $\mu(FMX)$. In other words, $\mu(FMX)$ cannot be scheduled in the middle of these two data operations. Notice that the Join operator is the earliest ancestor one-to-many operator of the reconfiguration operator FMX . If an FCM is sent to an operator O after the Join operator, since the operator O could possibly generate multiple data operations for the same data transaction, the FCM can be injected in the middle of these data operations, causing the schedule to be not conflict-serializable. Based on these observations, to guarantee the conflict-serializability, we can start the synchronization from the Join operator using an epoch marker. Recall that the Fries scheduler starts the epoch marker propagation from the head operators of a component in the MCS. The MCS is constructed using a set of operators M , which includes the reconfiguration operator FMX . To make sure the Join operator is treated as a head operator in a component, we add the operator to M before computing the MCS.

Algorithm 3 The Fries Scheduler (for general dataflows with one-to-many operators)

Input: A dataflow $G = (V, E)$

Input: A reconfiguration $\mathcal{R} = \{(o_1, U_1), \dots, (o_n, U_n)\}$

1: $M = \{o_1, \dots, o_n\}$

2: **for** each reconfiguration operator o_i in $\{o_1, \dots, o_n\}$ **do**

3: $\mathcal{A} \leftarrow$ set of ancestor one-to-many operators of o_i

4: $\mathcal{E} \leftarrow \text{computeEarliestAncestors}(\mathcal{A})$

5: $M \leftarrow M \cup \mathcal{E}$

6: ... same as Algorithm 2 line 2-6

Algorithm 3 shows the extended Fries scheduler, with the part in the box showing the differences compared to the original Fries scheduler in Algorithm 2. When constructing the MCS, apart from adding the operators in the reconfiguration to M (line 1), we also add to M all the earliest one-to-many ancestor operators of each reconfiguration operator o_i (lines 2 to 5). This step is done by first finding the set of ancestor one-to-many operators of o_i , denoted as \mathcal{A} , then finding the earliest ones in \mathcal{A} . Notice that a reconfiguration operator could have more than one earliest ancestor one-to-many operator. For example, in Figure 8, suppose the operators FMX and FMY are the only one-to-many operators in the dataflow. Then the reconfiguration operator U has both FMX and FMY as its earliest ancestor one-to-many operators according to the partial order of the DAG. We do the modification in the box because we want to

start the synchronization from these one-to-many operators with the reconfiguration operators using epoch markers. The remaining steps are the same as in Algorithm 2.

As an example, in Figure 8, the only one-to-many operator is the Join operator J . Because the reconfiguration operator FMX 's earliest ancestor one-to-many operator is J , we add J to M when constructing the MCS. The resulting MCS includes a single component with operators J , SP , and FMX , together with their edges. The controller injects an FCM to operator J , which propagates an epoch marker within the component to operator FMX .

We show that the extended Fries scheduler still guarantees conflict-serializability of its produced schedule.

LEMMA 6.1. (Corresponding to Lemma 5.6.) *Consider a dataflow graph G with a reconfiguration \mathcal{R} , and the MCS G' generated by Algorithm 3. Each component of G' contains at least one reconfiguration operator.*

PROOF. Let M be the set of operators used in Algorithm 3 to compute the MCS in line 1. Using steps similar to those in Lemma 5.6, we can show each component contains at least one operator in M . By the construction in Algorithm 3, an operator P in M is either (1) a reconfiguration operator, or (2) an earliest one-to-many ancestor operator of a reconfiguration operator O . In the latter case, by the construction in Algorithm 3, O is also in G' . By the definition of components, O is in the same component as P . Therefore, in both cases, each component of G' contains at least one reconfiguration operator. \square

LEMMA 6.2. (Corresponding to Lemma 5.7.) *Consider a dataflow graph G with a reconfiguration \mathcal{R} , and the MCS G' generated by Algorithm 3. For each source tuple, the operators in its data transaction overlap with at most one component of G' .*

PROOF. Suppose the operators processing a tuple t overlap with two components C_1 and C_2 in the MCS. By Lemma 6.1, there is a reconfiguration operator A in C_1 and another reconfiguration B in C_2 . Let $(\mathcal{S}, \preceq_{\mathcal{S}})$ be the scope of t . Let t_A and t_B be two tuples (in \mathcal{S}) processed by operators A and B , respectively. Notice that the partial order $\preceq_{\mathcal{S}}$ of the scope forms a tree. Let t_L be the latest common ancestor tuple of t_A and t_B in the tree. By the definition of the scope $(\mathcal{S}, \preceq_{\mathcal{S}})$, the receiving operator L of t_L must be a one-to-many operator because there is more than one child of t_L in the tree. Notice that L is a common ancestor of A and B because it has paths to both operators in G . For operator A , by the construction in Algorithm 3, L is either (1) an earliest one-to-many operator of A , or (2) on the path between A and an earliest one-to-many operator of A . In both cases, L is in G' . By the definition of components, since L is in G' and L is connected to both A and B , A and B must be in the same component of G' , which contradicts the assumption. \square

LEMMA 6.3. *Consider a dataflow graph G with a reconfiguration \mathcal{R} , and the MCS G' generated by Algorithm 3. A head operator H in a component of G' receives at most one input tuple.*

PROOF. Let M be the set of operators used in 3 to compute the MCS. Suppose a head operator H of a component in G' is not in M . We construct a new sub-DAG G'' by removing S and its edges from G' . Using similar steps as in Lemma 5.5, we can show that G''

is still a minimal covering sub-DAG of G and M , which contradicts the minimality property of G' .

By the construction in Algorithm 3, operator H is either (1) a reconfiguration operator with no ancestor one-to-many operators, or (2) an earliest one-to-many operator of a reconfiguration operator, which also has no ancestor one-to-many operators. Therefore, H can receive at most one input tuple in T . \square

THEOREM 6.4. (Corresponding to Theorem 5.8.) *For a workflow possibly with one-to-many operators and a reconfiguration request, Algorithm 3 always produces a conflict-serializable schedule.*

PROOF. Consider the function-update transaction U of a reconfiguration \mathcal{R} in the algorithm and the data transaction T for a source tuple t . Lemma 6.2 shows that the operators in T overlap with at most one component of the MCS G' produced in the algorithm. Consider a head operator H in a component of G' . Lemma 6.3 shows that a head operator H in a component of G' can receive at most one input tuple in T . We compare the position of the epoch marker on H with a possible single input tuple of H to determine the position of T in a serial schedule. We can prove this claim using steps similar to those in the proof of Theorem 5.8. \square

6.3 Reducing delay by MCS pruning

For dataflows with one-to-many operators, the reconfiguration delay can be long when there are many intermediate operators between the head of an MCS component and a reconfiguration operator in the component. To address this limitation, we improve the Fries scheduler in Algorithm 3 by using pruning rules to remove one-to-many operators that do not need to be synchronized. Algorithm 4 shows the addition of a pruning step. In line 4, we call a function `pruneAncestors` that applies pruning rules to each of the ancestor one-to-many operators to decide it can be pruned.

Algorithm 4 The Fries Scheduler with a Pruning Process

```

1:  $M = \{o_1, \dots, o_n\}$ 
2: for each reconfiguration operator  $o_i$  in  $\{o_1, \dots, o_n\}$  do
3:    $\mathcal{A} \leftarrow$  set of ancestor one-to-many operators of  $o_i$ 
4:   pruneAncestors( $\mathcal{A}$ )
5:    $\mathcal{E} \leftarrow$  computeEarliestAncestors( $\mathcal{A}$ )
6:    $M \leftarrow M \cup \mathcal{E}$ 
7: ... same as Algorithm 2 line 2-6

```

Next, we introduce two pruning rules that are used in the improved Fries scheduler.

1. Edge-wise one-to-one pruning rule. Figure 9 (I) shows a part of a dataflow with a Replicate operator, denoted as RE . This operator replicates each input tuple to produce two output tuples and sends each of them to operators C and D . RE is a one-to-many operator by Definition 5.2. Suppose all other operators in this dataflow are one-to-one operators. Using Algorithm 3, the Fries scheduler includes operators RE , C , and E in the MCS, as shown in the red box in Figure 9 (I). This is because RE is the earliest one-to-many ancestor operator of the reconfiguration operator E .

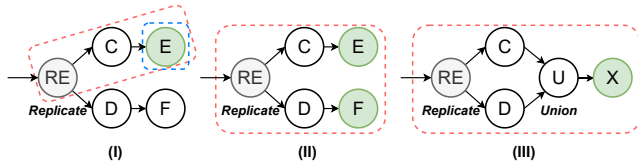


Figure 9: Example reconfigurations on dataflows with a replicate operator. (I): The MCS can be pruned. (II) and (III): the MCS's cannot be pruned.

Although operator RE is a one-to-many operator, for an input tuple, the operator outputs a single tuple on each edge. For the reconfiguration operator E , it only receives a single tuple in each data transaction. Therefore, there is no need for operator E to synchronize with operator RE . The MCS only contains operator E , as shown in the blue box in Figure 9. Figure 9 (II) and (III) show dataflows where the MCS with a replicate operator cannot be pruned. In Figure 9 (II), for each tuple processed by operator E , the corresponding replicated tuple must be processed by the same version of operator F . We can achieve the goal by starting the synchronization from RE . In Figure 9 (III), operator X receives all the replicated tuples in each data transaction. Therefore we also need to start the synchronization from the one-to-many operator RE .

Next, we formally describe the pruning rule. We prune an ancestor one-to-many operator A of a reconfiguration operator o_i if the following conditions are true. (1) On each of its output edges, A emits at most one tuple for each input tuple. (2) The A has only one output edge e connected to a downstream reconfiguration operator, and this output edge e is connected to o_i . Intuitively, condition (1) ensures that A behaves like a one-to-one operator on each of its output edges. Condition (2) ensures that the reconfiguration transaction of o_i affects only one output tuple of A sent on edge e . As analyzed in Section 6.2, a one-to-many operator O needs to be included in the MCS to ensure multiple output tuples of O are processed using the same configuration. In this case, only a single output tuple of A is affected by the reconfiguration. Therefore, A can be pruned from the set of operators used to construct the MCS.

2. Uniqueness pruning rule.

Next, we show another example of pruning a one-to-many operator. In Figure 10, suppose we want to reconfigure operator E . Each input tuple is first replicated by operator RE . The replicated tuples are sent to operators C and D . They are then combined to a single tuple using a Self-Join operator SJ on the primary key. Algorithm 3 computes the sub-DAG from operator RE to operator E as the MCS, as shown in the red box in Figure 10. However, notice that operator SJ ensures that it generates at most one output tuple for input tuple from the source. Therefore, RE does not need to be synchronized and the MCS only needs to contain E without RE , as shown in the blue box. In general, we prune an ancestor one-to-many operator A of a reconfiguration operator o_i if on each path from A to o_i , there exists an operator O that has the following uniqueness property: operator O generates at most one output tuple for each data transaction. In the running example, SJ is such an O operator and RE can be pruned.

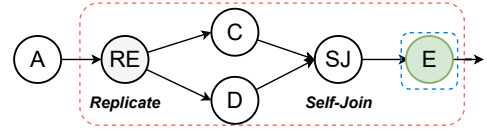


Figure 10: Operator RE can be pruned from the set of operators used to construct the MCS.

7 EXTENSIONS

In this section, we consider how the Fries scheduler works in more general cases, including the case of workflows with blocking operators and the case where an operator has multiple workers. Moreover, we discuss how to support fault tolerance in the Fries scheduler.

7.1 Dataflows with Blocking Operators

We now consider how the Fries scheduler works on dataflows containing blocking operators, such as aggregation and sort. Consider a blocking operator B . All operators before B need to run to their completion before the operators after B start to run. In other words, the operators before B and those after B never execute at the same time. Based on this observation, we can use the blocking operators in a dataflow to divide the dataflow into multiple sub-dataflows, with each of them containing pipelined operators only. Then we run Fries on each sub-dataflow during its execution.

7.2 Multiple Workers for an Operator

In a parallel execution engine, each operator can have multiple workers, with each worker processing a data partition. We map a single-worker dataflow $G = (V, E)$ to a parallel dataflow $G^* = (V^*, E^*)$, where each operator v in V is mapped to multiple parallel workers v^1, \dots, v^p in V^* , where p is the number of workers of the operator. We map a reconfiguration \mathcal{R} specified on the single worker dataflow G to a new reconfiguration \mathcal{R}^* on the parallel dataflow G^* of G . Figure 11 shows part of a parallel dataflow based on Figure 8, where each operator runs using two workers. For each function update $\mu(o_i)$ on an operator o_i in R , we map it to a set of function updates on all the workers of o_i , i.e., $\{(o_i^1, \mu(o_i)), \dots, (o_i^p, \mu(o_i))\}$ in R^* . For example, the reconfiguration on operator FMX is mapped to a reconfiguration on the corresponding workers FMX_1 and FMX_2 .

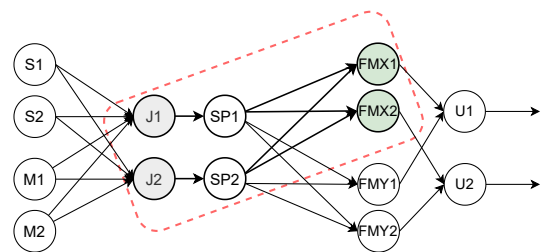


Figure 11: A reconfiguration on a parallel dataflow with two workers per operator.

Notice that the parallel dataflow G^* is also a DAG. The Fries scheduler in Algorithm 4 can be directly run on G^* with \mathcal{R}^* . The

operators and edges in the generated MCS are highlighted in red in Figure 8. The Fries scheduler treats a worker of an operator to have the same property (one-to-one or one-to-many) as the operator in hash and range partitioning. For example, both workers of the Join operator are treated as one-to-many operators. When using the broadcast strategy, a worker broadcasts an output tuple to all its downstream operators, same as the Replicate operator described in Section 6.3. In this case, the Fries treats it as if a Replicate operator is added after the worker. The pruning techniques described in Section 6.3 can still be used.

7.3 Fault Tolerance Using the Fries Scheduler

Fault tolerance requires that a system can recover to a consistent state in case of failures. For a dataflow G and a reconfiguration \mathcal{R} , the execution of the dataflow is not in a consistent state if some operators in \mathcal{R} are updated, and some operators in \mathcal{R} are not. In an epoch-based scheduler, fault-tolerance can be supported using epoch-based checkpointing [6, 7]. However, such checkpointing cannot guarantee fault tolerance for the Fries scheduler. Consider the reconfiguration in Figure 7 and the following sequence of events: (1) G receives a checkpoint marker from B ; (2) G and C receive the reconfiguration FCM's; and (3) C receives a checkpoint marker from A . The checkpoint contains the old configuration of G and the new configuration of C , which is not in a consistent state. Next we discuss two methods to support fault tolerance in Fries.

Checkpoint-based fault tolerance. When a reconfiguration request arrives at the controller, the controller cancels all in-flight checkpoints because they could produce inconsistent states. The controller then blocks any new checkpoints to be started until all head operators of each MCS component have received their FCM's. In this way, the subsequent epoch markers will always be after the FCM's, thus the subsequent checkpoints only contain the fully updated configuration. The blocking period is short because the FCM's are not blocked by any data messages.

Logging-based fault tolerance. The FCMs introduce non-determinism in the execution of an operator. We can log all the non-determinism factors of each operator, including the arrival order of data tuples and the FCMs. During recovery, each operator is deterministically replayed and the FCMs are injected following the original order. We can leverage an existing logging-based fault-tolerance approach such as the one in Clonos [31], which is built on top of Flink. FCMs can be modeled as RPC calls received by an operator in Clonos, which are recorded in the logs.

8 EXPERIMENTS

In this section, we present the results of experiments of different reconfiguration schedulers and show the benefits of Fries.

8.1 Setting

Datasets. We used three datasets shown in Table 3. Dataset 1 had 24M tuples of credit card payments with 12 attributes [29], such as the customer, merchant, date, amount, and chip usage. Dataset 2 was constructed by grouping the credit card payments per user in dataset 1. Each record had a user and a list of payments by the user. We used this dataset to utilize a one-to-many unnest operator to

split a payment list into multiple records. Dataset 2 was generated using the TPC-DS benchmark [35] with a scale factor of 100.

Workflows. We constructed workflows as shown in Figure 12. Workflow W_1 simulated a fraud detection application, and it detected fraud of a user based on the user's historical payment amounts. By default, the source operator read the payment table with a rate of 1,000 tuple/s. The user-based inference operator saved 10 most recent payment amounts for each user as its internal state. For each input tuple, the operator updated the user's state and used an LSTM auto-encoder [38] to predict the probability of fraud. Workflow W_2 was constructed based on TPC-DS query 40. For all items with a price between 0.99 and 1.49, this workflow computed the item id and location of the warehouse the item was delivered from in a 60-day period. Workflow W_3 was constructed based on TPC-DS query 71. It produced the brands managed by a given manager that sold their products across three sales channels at either breakfast or dinner time for a given month. All the join operators in these workflows were one-to-one operators because they join a primary key with a foreign key. We only considered the pipelined sub-DAG of each dataflow. For example, if a hash join has a build phase and a probe phase, we only consider the pipelined probe phase. In Figure 12, we highlighted all the pipelined edges considered in the experiment in red.

On top of W_1 , workflow W_4 included an additional merchant-based inference operator for users who made a large amount of payments. For each merchant, the inference operator saved 50 most recent payments, and used a similar LSTM auto-encoder to do inference. A payment record was processed by both inference operators. If one of them produced a probability greater than a threshold, the payment record was flagged as fraud. Workflow W_5 replicates the payment tuples to both the user-based inference operator and the merchant-based operator. After each operator makes fraud predictions, a Self-Join operator is used to combine the replicated tuples into a single one.

Dataset	Table	Attribute #	Tuple #
1	Credit card payment	12	24M
2	Credit card payment aggregated per user	2	20K
3	Catalog sales	34	144M
	Store sales	23	288M
	Web sales	34	71M

Table 3: Datasets used in the experiments.

Reconfigurations. For workflow W_1 , we performed configurations with one operator. For workflows W_2 , W_3 , and W_4 , we performed reconfigurations with multiple operators. The methods of choosing reconfiguration operators will be described in each experiment.

Schedulers. We implemented two epoch-based schedulers. The first one performed a reconfiguration with a savepoint, which was natively supported by Flink (described in Section 3). The second one was the scheduler of Chi [24] (described in Section 3). As Chi was not open source, we implemented this scheduler on top of Flink, and used Flink's aligned checkpoint barriers as epoch markers. The first scheduler always stopped and restarted the execution *after* the propagation of checkpoint barriers to apply reconfiguration. The second scheduler applied reconfiguration *during* the barrier

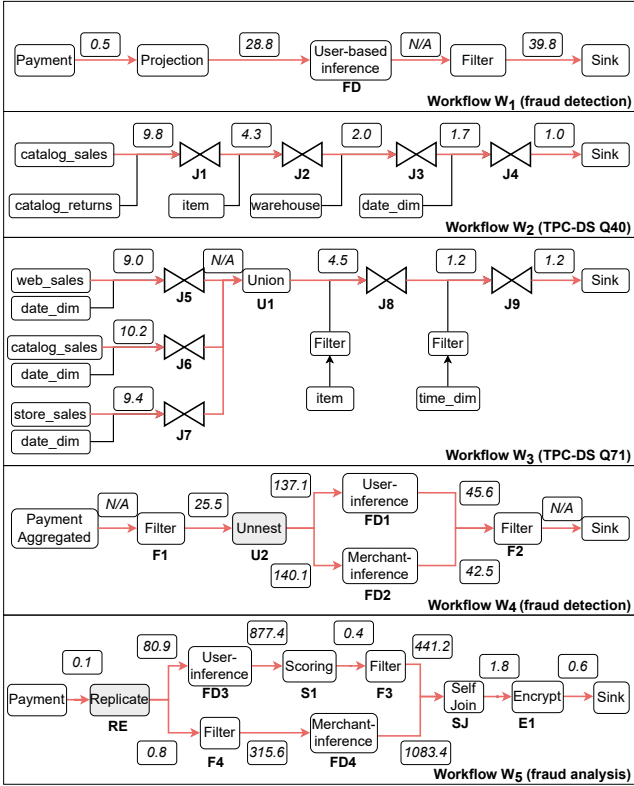


Figure 12: Workflows used in the experiments. Pipelined edges are highlighted in red.

propagation, and did not require an additional stop-and-restart of the system. As a consequence, the second scheduler always had a shorter reconfiguration delay than the first, as verified in our experiments. Therefore, between these two schedulers, we only report the results of the second, denoted as “Epoch scheduler.”

For fair-comparison purposes, we implemented Fries also on top of Flink. In the implementation, FCM’s between the controller and a specific worker of an operator were sent in special network channels (available in Flink). For each MCS C computed in Fries for a reconfiguration, the controller sent FCM’s to the workers of C ’s head operators. These workers pushed checkpoint barriers to the workers of their downstream operators in C . To let every operator know which downstream operators were in C , the checkpoint barrier also included C and the reconfiguration operators in C . Every reconfiguration operator in C applied the reconfiguration after receiving checkpoint barriers from all its upstream operators in C . The reconfiguration for this MCS C completed after all C ’s reconfiguration operators applied the reconfiguration.

System environment. All the experiments were conducted on the Google Cloud Platform (GCP). The execution was on a GCP dataproc cluster with 1 coordinator machine and 10 worker machines. All the machines were of type n1-highmem-4 with Ubuntu 18.04. The job controller of Flink ran on the coordinator. The coordinator machine had a 2TB HDD, while each worker machine had a 250GB HDD. To separate computation and storage, we stored the datasets

in an HDFS file system on another cluster with 6 e2-highmem-4 machines, each with 4 vCPU’s, 32 GB memory, and a 500GB HDD. For all the schedulers, we used Flink release 1.13 and Java 8.

8.2 Choke Point Analysis of Workflows

In the execution there were various choke points in the workflow where the reconfiguration delay between two operators was very high. We analyzed these choke points in the experiment workflows by computing the average reconfiguration delay between two operators using the epoch scheduler and showed the numbers on top of each edge in Figure 12. The numbers represented the delay from the time when the upstream operator applied the reconfiguration and sent checkpoint barriers to the time when the downstream operator aligned all the checkpoint barriers and applied the reconfiguration. Some edges are marked as N/A because the two connected operators were fused to a single operator chain in Flink. Edges marked with a number perform re-partition operations, thus the two connected operators are not chained.

We had the following observations. 1) Expensive operators usually created choke points in the workflow. For example, in W4, both inference operators applied the reconfiguration from U1 after the checkpoint barriers were sent out for around 140s. The inference operators accumulated input tuples in their input data channel, which blocked the checkpoint barrier to be processed. 2) Stragglers also created choke points. For example, in W5, there was a delay of 877.4s between FD3 and S1, because one of the FD3 workers was a straggler. Recall that due to the epoch alignment step, S1 had to receive all the checkpoint barriers before applying the reconfiguration. S1 was blocked when waiting for the straggler FD3 worker to finish. 3) If operators had similar costs, choke points depended on the amount of data in each operator’s input data channel. For example, in both W2 and W3, the first several joins had larger delays of reconfiguration. This is because the data was filtered by every join, and the joins near the sink received less data so they had a lower reconfiguration delay.

8.3 Benefits of Short Reconfiguration Delay: Reducing End-to-end Tuple Latency

A main advantage of Fries was its short reconfiguration delay compared to epoch-based schedulers. To show the benefits of this advantage, we considered a scenario for W1 as shown in Figure 13, where the developer needed to hot-replace the model in the user-based inference operator FD during the execution to deal with a sudden surge of input data. In W1, we set the number of workers for operators (except for the source and sink) to 40 to utilize all the cores in the cluster. The time for FD to process a tuple was about 25ms, and the maximum throughput of this operator was around 1,600 tuple/s. We used a single worker of the source operator and another single worker of the sink operator on the same machine so that they can use the same clock. The source operator started with an initial ingestion rate of 1,000 tuples/s. After 100 seconds, we increased the ingestion rate to 2,000 tuples/s. The developer saw an increasing trend of the end-to-end tuple latency. He requested a reconfiguration to replace the original LSTM auto-encoder model in FD with another LSTM auto-encoder with fewer parameters at $t = 120$ s to speed up the processing. The developer continuously

monitored the end-to-end tuple latency. After another 100 seconds, we further increased the rate to 9,000 tuples/s. The developer decided to further decrease the cost of *FD* to reduce the latency. At $t = 220$ s, he requested another reconfiguration to replace the LSTM auto-encoder model with a simple decision-tree model.

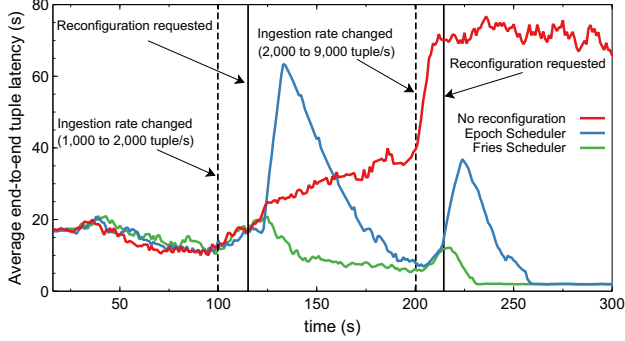


Figure 13: Effect of mitigating surges of data-ingestion rate by different schedulers (W_1 on dataset 1).

To compute the end-to-end latency of each input tuple, we attached a timestamp at the moment when the source operator generated this tuple. When the tuple was received by the sink operator, the latency was computed as the difference between the current time and the attached timestamp. Figure 13 shows the average end-to-end latency of output tuples received for every 10-second sliding window. (1) For the case without reconfiguration, after 100 seconds, the end-to-end latency began to increase because *FD* was not fast enough to process all the incoming tuples. Many tuples were buffered in the network channel. The latency increased continuously and stabilized at around 70s when backpressure from *FD* was propagated to the source operator to slow down the data ingestion rate. (2) For the case of using the Epoch scheduler, the latency rapidly increased to above 60 seconds until around $t = 135$ s due to the surge. The main reason for the increase in the end-to-end latency was the blocking in the epoch alignment step. Since the sink operator had only one worker, it needed to wait until all 40 upstream *FD* workers completely processed all tuples in the old epoch before it could process any tuples in the new epoch. Note that the delay was determined by the slowest *FD* worker. We observed that the average delay of all workers was 30 seconds. However, there were two straggler workers that took 58 seconds and 69 seconds to finish processing the old epoch, respectively. The two straggler workers suffered from data skew. On average, each worker processed 35,000 tuples in the old epoch. However, the slowest worker processed 62,000 tuples.

(3) For the case of using the Fries scheduler, the latency immediately decreased after $t = 120$ s, indicating that *FD* applied the reconfiguration and was able to quickly process the buffered tuples. Compared to Epoch, Fries required less time to mitigate the surge. In this reconfiguration, the MCS component contained operator *FD* only. Therefore, FCMs are directly sent to all *FD* workers and no epoch markers were propagated to any downstream operators. This eliminated the aforementioned delay caused by the epoch alignment step.

8.4 Benefits of Short Reconfiguration Delay: Reducing Wasted Computing Resources

Another benefit of a short reconfiguration delay can be illustrated in the following scenario. When processing data with unexpected content or formats, the workflow can produce invalid output tuples to be collected and reprocessed. A large number of invalid output tuples not only wastes computation in the current execution, but also requires more resources in the future. A short reconfiguration delay can effectively reduce the amount of wasted computing resources. To illustrate the benefit, we considered workflow W_1 , and attached a version number V_1 to every source tuple. The user-based inference operator *FD* had another version number V_2 for its processing logic. For every input tuple, *FD* expected V_1 of the tuple to match with V_2 ; otherwise, the operator produced an invalid output tuple. For every 50 seconds, we increased V_1 , and the developer realized the version changed 20 seconds after that. Then, he requested a reconfiguration of *FD* to also increase its version V_2 . We measured the number of invalid output tuples produced by the workflow over time under different reconfiguration schedulers as a metric of wasted computing resources.

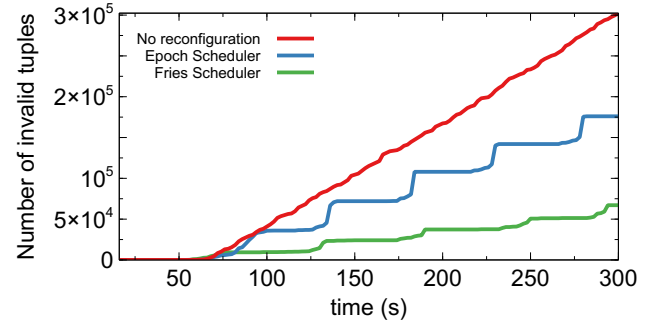


Figure 14: Effect of schedulers on the number of invalid output tuples (W_1 on dataset 1).

Figure 14 showed the result. (1) For the case without reconfiguration, all the output tuples after the first input version update were invalid. Thus the number of invalid tuples increased continuously. After 300 seconds, the number of invalid tuples reached 302K. (2) For the case of using the Epoch scheduler, operator *FD* had to process all the tuples prior to the epoch marker before applying the reconfiguration. So all the tuples after the input version update and prior to the marker were invalid. The workflow produced many invalid tuples after each input version update, resulting in reprocessing of 176K tuples after 300 seconds. (3) For the case of using the Fries scheduler, the operator quickly applied the reconfiguration, so fewer invalid tuples were generated for each input version change. At the end, only 67K tuples needed to be reprocessed.

8.5 Effect of Data Ingestion Rates on Reconfiguration Delays

Next we evaluated the effect of different factors on the delay. We first considered data-ingestion rate. For workflow W_1 , we gradually increased the rate at the source operator from 500 tuples/s to 2,500 tuples/s. For each configuration, after the execution of 120 seconds,

we applied a dummy reconfiguration on operator FD and measured the delay under the two schedulers. As shown in Figure 15 (with a log scale for the y -axis), when the ingestion rate increased, the delay of the Epoch scheduler also increased due to the larger amount of in-flight tuples prior to the epoch marker. Since the Fries scheduler sent FCM’s directly to FD , its delay grew much slower than the Epoch scheduler.

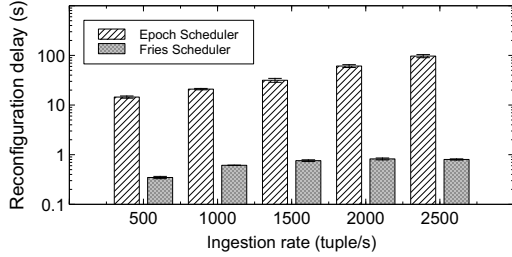


Figure 15: Effect of data ingestion rate on the reconfiguration delay (with 95% confidence intervals) (W_1 on dataset 1).

8.6 Effect of Operator Costs on Delays

To evaluate the effect of operator cost on the reconfiguration delay, for workflow W_1 , we gradually increased the cost of the user-based inference operator FD to process each input tuple. The FD operator maintained a bounded queue of recent payment amounts of each user. When an input tuple was received by FD , the operator passed the payment amounts in the queue to its ML model. In different runs of experiments, we gradually increased the size of this queue from 10 to 50 so that the operator took more time to process each input tuple. Again, for each configuration, after the execution ran for 120 seconds, we applied a dummy reconfiguration on FD and measured the delay under the two schedulers. As shown in Figure 16, when the FD ’s cost increased, the delay of the Epoch scheduler also increased because each in-flight data tuple prior to the epoch marker took more time to be processed. On the other hand, the delay of the Fries scheduler grew much slower than the Epoch scheduler.

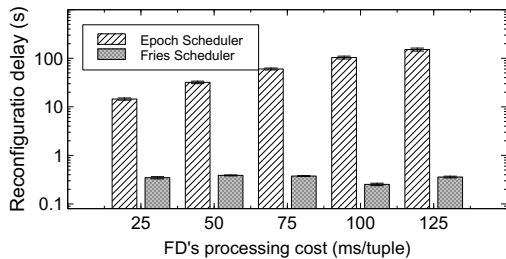


Figure 16: Effect of operator cost on the reconfiguration delay with 95% confidence intervals (W_1 on dataset 1).

8.7 Effect of Reconfigurations on Delays

We wanted to evaluate the effect of reconfigurations on the delay under the two schedulers. We varied the number of reconfiguration operators in both workflows W_2 and W_3 . For both workflows,

we used 40 workers for each operator. For every 10 seconds, we requested a reconfiguration and measured the average reconfiguration delay. The results are shown in Table 4. For each reconfiguration, we show its operators, the MCS components generated by the Fries scheduler, the length of a longest path of each component, the delay of using the Fries scheduler, and the delay of using the Epoch scheduler. We reported the path length because it affected the delay in the Fries scheduler.

We have the following observations from the results. (1) The delay of the Fries scheduler was always significantly lower than the delay of the Epoch scheduler. For example, for the W_2 configuration including $J1$ and $J4$, the delay of the Fries scheduler was 1,702ms, compared to 12,361ms of the Epoch scheduler. (2) For reconfigurations with multiple operators, if each operator formed a component in MCS, the delay of Fries was very low. For example, for the W_3 reconfiguration of $J5$ and $J6$, each of them formed their own component. The Fries scheduler had a delay of 127ms, comparable to 87ms in the case with $J5$ as the only reconfiguration operator. This low delay was because the Fries scheduler sent FCM’s separately to both operators and their reconfiguration happened in parallel. (3) When the length of the longest path in a component increased, as expected, the delay of the Fries scheduler also increased. For example, for the reconfiguration of $J1$ and $J3$, the longest path in their MCS had a length of 2, and the delay was 1,664ms. For the reconfiguration of $J1$ and $J4$, the longest path in their MCS had a length of 3, and the delay increased to 1,702ms.

Workflow	Reconfiguration operators	MCS components	Longest path length	Fries Scheduler delay (ms)	Epoch Scheduler delay (ms)
W_2	$J1$	{J1}	0	46	11,432
	$J2$	{J2}	0	44	11,709
	$J1, J3$	{J1, J2, J3}	2	1,664	12,339
	$J1, J4$	{J1, J2, J3, J4}	3	1,702	12,361
	$J3, J4$	{J3, J4}	1	387	13,767
W_3	$J5$	{J5}	0	87	4,127
	$J5, J6$	{J5}	0	127	8,352
	$J5, J6, J7, J8$	{J5, J6, J7, U1, J8}	3	447	19,608
	$J5, J6, J7, J9$	{J5, J6, J7, U1, J8, J9}	4	526	19,717
	$J7, J8, J9$	{J7, U1, J8, J9}	3	1,340	20,532

Table 4: Reconfiguration operators, corresponding MCS, and reconfiguration delay in W_2 and W_3 on dataset 3. Head operators in each component are highlighted in bold.

8.8 Reconfiguration Delays in Workflows with One-to-many Operators

We used workflow W_4 to evaluate the effect of reconfiguration operators on the reconfiguration delay in workflows with a one-to-many operator $U2$. This operator split all the payments of a user and sent them to both $FD1$ and $FD2$. Table 5 shows the results. We have the following observations. (1) The delay of the Fries scheduler was still always lower than the Epoch scheduler. (2) The reconfiguration of $FD1$ took a long time (47,892ms) in Fries because $FD1$ was not the head operator of its component. The epoch markers had to go

through the data channels of $FD1$ (from multiple workers). Since $FD1$ processed tuples slowly, many of its input tuples were buffered in its data channels, which delayed the propagation of the epoch markers. (3) The reconfiguration of $F2$ took a long delay (221, 353ms) in Fries because its generated MCS contained every operator on the path from $U2$ and $F2$ with the one-to-many $U2$ operator and both $FD1$ and $FD2$ were slow.

Reconfiguration operators	MCS components	Longest path length	Fries Scheduler delay (ms)	Epoch Scheduler delay (ms)
F1, U2	{ F1 , U2}	1	69	151
FD1	{U2, FD1 }	1	47,892	131,103
F2	{U2, FD1 , FD2 , F2 }	5	221,353	236,153

Table 5: Reconfiguration operators, corresponding MCS, and reconfiguration delay in W_4 on dataset 2. Head operators in each component are highlighted in bold.

8.9 Effect of MCS Pruning on Delays in Workflows with One-to-many Operators

We used workflow W_5 to evaluate the effect of the MCS pruning method proposed in Section 6.3 on the reconfiguration delay in workflows with a one-to-many Replicate operator and a Self Join operator. For each reconfiguration, we compare the Fries scheduler with the pruning step turned on and turned off. Table 6 shows the results. We have the following observations. (1) In general, when pruning is possible, the size of MCS components was reduced and the delay with pruning was significantly lower than the delay without pruning. For example, the reconfiguration of operator $FD4$ and the reconfiguration of operator $F3$ benefited from the edge-wise one-to-one pruning rule. (2) In the case of reconfiguring both $FD3$ and $FD4$, the pruning rules could not prune the one-to-many Replicate operator. Therefore the delays were similar. (3) The reconfiguration of operator $E1$ benefited from the uniqueness pruning rule. This reconfiguration had the largest benefit in delay because the number of edges in the MCS reduced from eight to zero, which greatly reduced the synchronization time.

8.10 Effect of Multiple Workers on Delays

To evaluate the effect of the worker number per operator on the reconfiguration delay, we considered workflow W_2 and increased the worker number per operator from 1 to 40. After the workflow ran for 20 seconds, we requested a dummy reconfiguration of $J1$ and $J4$. We measured the reconfiguration delay of the two schedulers.

Reconfiguration operators	MCS with pruning	MCS without pruning	Fries with pruning delay (ms)	Fries without pruning delay (ms)
FD4	{ FD4 }	{ RE , F4, FD4}	158	450,149
F3	{ F3 }	{ RE , FD3, S1, F3}	94	383,781
F4	{ F4 }	{ RE , F4}	10	446
FD3, FD4	{ RE , FD3, F4, FD4}	{ RE , FD3, F4, FD4}	661,892	663,460
E1	{ E1 }	{ RE , FD3, S1, F3, F4, FD4, SJ, E1}	85	1,122,686

Table 6: The effect of MCS pruning on delays in W_5 .

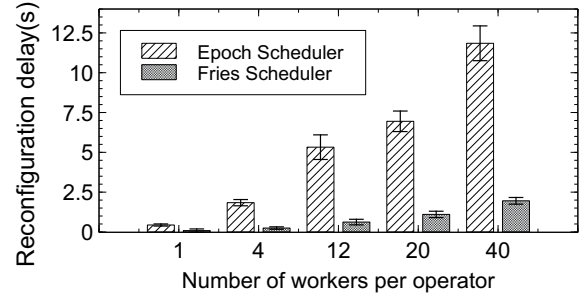


Figure 17: Effect of worker number on reconfiguration delay with 95% confidence intervals (W_2 on dataset 3).

As shown in Figure 17, as the worker number increased, the delay increased for both schedulers. This was because between each pair of join operators, the data was shuffled and every join worker needed to receive an epoch marker from all its upstream workers. So the number of data channels between the joins was the product of their numbers of workers. When each worker number increased, the number of epoch markers to collect also increased. The fact that the delay of Fries scheduler was again lower than the Epoch scheduler can be explained using Table 7. In particular, the Fries scheduler propagated epoch markers only through the data channels between MCS workers, while the Epoch scheduler had to propagate epoch markers through all the data channels. The table shows that the number of channels between MCS workers was always less than the number of channels between all workers.

Worker # per operator	Total # of data channels between all workers	Total # of data channels between MCS workers
1	5	3
4	68	48
12	588	432
20	1,620	1,200
40	6,440	4,800

Table 7: Effect of number of workers on data channels for reconfiguration of $J1$ and $J4$ (W_2 on dataset 3).

9 CONCLUSIONS

In this paper we studied the problem of runtime configurations in data-intensive workflow systems with a low delay. We showed limitations of existing epoch-based reconfiguration schedulers on the delay. We developed a new technique called Fries that uses fast control messages to do reconfigurations. We formally defined consistency in runtime reconfigurations, and developed a Fries scheduler with consistency guarantee. The technique also works for parallel executions and supports fault tolerance. Our extensive experimental evaluation showed the advantages of this technique compared to epoch-based schedulers.

Acknowledgements: This work was supported by the NSF IIS-2107150 award. We thank Sadeem Alsudais and Yicong Huang for their participation in discussions.

REFERENCES

- [1] Tyler Akidau, Robert Bradshaw, Craig Chambers, Slava Chernyak, Rafael Fernández-Moctezuma, Reuven Lax, Sam McVeety, Daniel Mills, Frances Perry, Eric Schmidt, and Sam Whittle. 2015. The Dataflow Model: A Practical Approach to Balancing Correctness, Latency, and Cost in Massive-Scale, Unbounded, Out-of-Order Data Processing. *Proc. VLDB Endow.* 8, 12 (2015), 1792–1803. <https://doi.org/10.14778/2824032.2824076>
- [2] Michael Armbrust, Tathagata Das, Joseph Torres, Burak Yavuz, Shixiong Zhu, Reynold Xin, Ali Ghodsi, Ion Stoica, and Matei Zaharia. 2018. Structured Streaming: A Declarative API for Real-Time Applications in Apache Spark. In *Proceedings of the 2018 International Conference on Management of Data, SIGMOD Conference 2018, Houston, TX, USA, June 10-15, 2018*, Gautam Das, Christopher M. Jermaine, and Philip A. Bernstein (Eds.). ACM, 601–613. <https://doi.org/10.1145/3183713.3190664>
- [3] Philip A. Bernstein, Vassos Hadzilacos, and Nathan Goodman. 1987. *Concurrency Control and Recovery in Database Systems*. Addison-Wesley. <http://research.microsoft.com/en-us/people/philbe/ccontrol.aspx>
- [4] Philip A. Bernstein and Eric Newcomer. 1996. *Principles of Transaction Processing for Systems Professionals*. Morgan Kaufmann.
- [5] Irina Botan, Peter M. Fischer, Donald Kossmann, and Nesime Tatbul. 2012. Transactional stream processing. In *15th International Conference on Extending Database Technology, EDBT '12, Berlin, Germany, March 27-30, 2012, Proceedings*, Elke A. Rundensteiner, Volker Markl, Ioana Manolescu, Sihem Amer-Yahia, Felix Naumann, and Ismail Ari (Eds.). ACM, 204–215. <https://doi.org/10.1145/2247596.2247622>
- [6] Paris Carbone, Stephan Ewen, Gyula Fóra, Seif Haridi, Stefan Richter, and Kostas Tzoumas. 2017. State Management in Apache Flink®: Consistent Stateful Distributed Stream Processing. *Proc. VLDB Endow.* 10, 12 (2017), 1718–1729. <https://doi.org/10.14778/3137765.3137777>
- [7] Paris Carbone, Gyula Fóra, Stephan Ewen, Seif Haridi, and Kostas Tzoumas. 2015. Lightweight Asynchronous Snapshots for Distributed Dataflows. *CoRR abs/1506.08603* (2015). [arXiv:1506.08603](http://arxiv.org/abs/1506.08603) <http://arxiv.org/abs/1506.08603>
- [8] Paris Carbone, Marios Fragkoulis, Vasiliki Kalavri, and Asterios Katsifodimos. 2020. Beyond Analytics: The Evolution of Stream Processing Systems. In *Proceedings of the 2020 International Conference on Management of Data, SIGMOD Conference 2020, online conference [Portland, OR, USA], June 14-19, 2020*, David Maier, Rachel Pottinger, AnHai Doan, Wang-Chiew Tan, Abdussalam Alawini, and Hung Q. Ngo (Eds.). ACM, 2651–2658. <https://doi.org/10.1145/3318464.3383131>
- [9] Paris Carbone, Asterios Katsifodimos, Stephan Ewen, Volker Markl, Seif Haridi, and Kostas Tzoumas. 2015. Apache Flink™: Stream and Batch Processing in a Single Engine. *IEEE Data Eng. Bull.* 38, 4 (2015), 28–38. <http://sites.computer.org/debull/A15dec/p28.pdf>
- [10] Badrish Chandramouli, Jonathan Goldstein, Mike Barnett, Robert DeLine, John C. Platt, James F. Terwilliger, and John Wernsing. 2014. Trill: A High-Performance Incremental Query Processor for Diverse Analytics. *Proc. VLDB Endow.* 8, 4 (2014), 401–412. <https://doi.org/10.14778/2735496.2735503>
- [11] Thomas H. Cormen. 2013. *Algorithms Unlocked*. MIT Press. <http://mitpress.mit.edu/books/algorithms-unlocked>
- [12] Sanjoy Dasgupta, Christos H. Papadimitriou, and Umesh V. Vazirani. 2008. *Algorithms*. McGraw-Hill.
- [13] Raul Castro Fernandez, Matteo Migliavacca, Evangelia Kalyvianaki, and Peter R. Pietzuch. 2013. Integrating scale out and fault tolerance in stream processing using operator state management. In *Proceedings of the ACM SIGMOD International Conference on Management of Data, SIGMOD 2013, New York, NY, USA, June 22-27, 2013*, Kenneth A. Ross, Divesh Srivastava, and Dimitris Papadias (Eds.). ACM, 725–736. <https://doi.org/10.1145/2463676.2465282>
- [14] FlinkFraudDetectionDemo [n.d.]. Advanced Flink Application Patterns Vol.1: Case Study of a Fraud Detection System, <https://flink.apache.org/news/2020/01/15/demo-fraud-detection.html>.
- [15] FlinkSavepoint [n.d.]. Savepoints in Apache Flink, <https://ci.apache.org/projects/flink/flink-docs-master/docs/ops/state/savepoints/>.
- [16] FlinkUpdateCepPattern [n.d.]. Support dynamically changing CEP patterns in Flink, <https://issues.apache.org/jira/browse/FLINK-7129>.
- [17] FlinkUpdateVol2 [n.d.]. Advanced Flink Application Patterns Vol.2: Dynamic Updates of Application Logic, <https://flink.apache.org/news/2020/03/24/demo-fraud-detection-2.html>.
- [18] Jon Gjengset, Malte Schwarzkopf, Jonathan Behrens, Lara Timbó Araújo, Martin Ek, Eddie Kohler, M. Frans Kaashoek, and Robert Tappan Morris. 2018. Noria: dynamic, partially-stateful data-flow for high-performance web applications. In *13th USENIX Symposium on Operating Systems Design and Implementation, OSDI 2018, Carlsbad, CA, USA, October 8-10, 2018*, Andrea C. Arpaci-Dusseau and Geoff Voelker (Eds.). USENIX Association, 213–231. <https://www.usenix.org/conference/osdi18/presentation/gjengset>
- [19] Moritz Hoffmann, Andrea Lattuada, Frank McSherry, Vasiliki Kalavri, John Liagouris, and Timothy Roscoe. 2019. Megaphone: Latency-conscious state migration for distributed streaming dataflows. *Proc. VLDB Endow.* 12, 9 (2019), 1002–1015. <https://doi.org/10.14778/3329772.3329777>
- [20] Konstantinos Kakousis, Nearchos Paspallis, and George Angelos Papadopoulos. 2010. A survey of software adaptation in mobile and ubiquitous computing. *Enterp. Inf. Syst.* 4, 4 (2010), 355–389. <https://doi.org/10.1080/17517575.2010.509814>
- [21] Fabio Kon and Roy H. Campbell. 1999. Supporting Automatic Configuration of Component-Based Distributed Systems. In *Proceedings of the 5th USENIX Conference on Object-Oriented Technologies & Systems, May 3-7, 1999, The Town & Country Resort Hotel, San Diego, California, USA*, Murthy V. Devarakonda (Ed.). USENIX, 175–188. <http://www.usenix.org/publications/library/proceedings/coots99/kon.html>
- [22] Avinash Kumar, Zuozhi Wang, Shengquan Ni, and Chen Li. 2020. Amber: A Debuggable Dataflow System Based on the Actor Model. *Proc. VLDB Endow.* 13, 5 (2020), 740–753. <https://doi.org/10.14778/3377369.3377381>
- [23] Xiaoxing Ma, Luciano Baresi, Carlo Ghezzi, Valerio Panzica La Manna, and Jian Lu. 2011. Version-consistent dynamic reconfiguration of component-based distributed systems. In *SIGSOFT/FSE'11 19th ACM SIGSOFT Symposium on the Foundations of Software Engineering (FSE-19) and ESEC'11: 13th European Software Engineering Conference (ESEC-13), Szeged, Hungary, September 5-9, 2011*, Tibor Gyimóthy and Andreas Zeller (Eds.). ACM, 245–255. <https://doi.org/10.1145/2025113.2025148>
- [24] Luo Mai, Kai Zeng, Rahul Potharaju, Le Xu, Steve Suh, Shivaram Venkataraman, Paolo Costa, Terry Kim, Saravanam Muthukrishnan, Vamsi Kuppa, Sudheer Dhulipalla, and Sriram Rao. 2018. Chi: A Scalable and Programmable Control Plane for Distributed Stream Processing Systems. *Proc. VLDB Endow.* 11, 10 (2018), 1303–1316. <https://doi.org/10.14778/3231751.3231765>
- [25] Yancan Mao, Yuan Huang, Runxin Tian, Xin Wang, and Richard T. B. Ma. 2021. Trisk: Task-Centric Data Stream Reconfiguration. In *SoCC '21: ACM Symposium on Cloud Computing, Seattle, WA, USA, November 1 - 4, 2021*, Carlo Curino, Georgia Koutrika, and Ravi Netravali (Eds.). ACM, 214–228. <https://doi.org/10.1145/3472883.3487010>
- [26] John Meehan, Nesime Tatbul, Stan Zdonik, Cansu Aslantas, Ugur Çetintemel, Jiang Du, Tim Kraska, Samuel Madden, David Maier, Andrew Pavlo, Michael Stonebraker, Kristin Tufte, and Hao Wang. 2015. S-Store: Streaming Meets Transaction Processing. *Proc. VLDB Endow.* 8, 13 (2015), 2134–2145. <https://doi.org/10.14778/2831360.2831367>
- [27] Bonaventura Del Monte, Steffen Zeuch, Tilmann Rabl, and Volker Markl. 2020. Rhino: Efficient Management of Very Large Distributed State for Stream Processing Engines. In *Proceedings of the 2020 International Conference on Management of Data, SIGMOD Conference 2020, online conference [Portland, OR, USA], June 14-19, 2020*, David Maier, Rachel Pottinger, AnHai Doan, Wang-Chiew Tan, Abdussalam Alawini, and Hung Q. Ngo (Eds.). ACM, 2471–2486. <https://doi.org/10.1145/3318464.3389723>
- [28] Derek Gordon Murray, Frank McSherry, Rebecca Isaacs, Michael Isard, Paul Barham, and Martin Abadi. 2013. Naiad: a timely dataflow system. In *ACM SIGOPS 24th Symposium on Operating Systems Principles, SOSP '13, Farmington, PA, USA, November 3-6, 2013*, Michael Kaminsky and Mike Dahlin (Eds.). ACM, 439–455. <https://doi.org/10.1145/2517349.2522738>
- [29] Inkit Padhi, Yair Schiff, Igor Melnyk, Mattia Rigotti, Youssef Mroueh, Pierre Dognin, Jerret Ross, Ravi Nair, and Erik Altman. 2021. Tabular transformers for modeling multivariate time series. In *ICASSP 2021-2021 IEEE International Conference on Acoustics, Speech and Signal Processing (ICASSP)*. IEEE, 3565–3569. <https://ieeexplore.ieee.org/document/9414142>
- [30] Alireza Sadeghi, Naem Eshfahani, and Sam Malek. 2017. Ensuring the Consistency of Adaptation through Inter- and Intra-Component Dependency Analysis. *ACM Trans. Softw. Eng. Methodol.* 26, 1 (2017), 2:1–2:27. <https://doi.org/10.1145/3063385>
- [31] Pedro F. Silvestre, Marios Fragkoulis, Diomidis Spinellis, and Asterios Katsifodimos. 2021. Clonos: Consistent Causal Recovery for Highly-Available Streaming Dataflows. In *SIGMOD '21: International Conference on Management of Data, Virtual Event, China, June 20-25, 2021*, Guoliang Li, Zhanhui Li, Stratos Idreos, and Divesh Srivastava (Eds.). ACM, 1637–1650. <https://doi.org/10.1145/3448016.3457320>
- [32] StreamINGFraudDetection [n.d.]. StreamING Machine Learning Models: How ING Adds Fraud Detection Models at Runtime with Apache Flink, <https://www.ververica.com/blog/real-time-fraud-detection-ing-bank-apache-flink>.
- [33] Abhishek Tiwari, Brian Ramprasad, Seyed Hossein Mortazavi, Moshe Gabel, and Eyal de Lara. 2019. Reconfigurable Streaming for the Mobile Edge. In *Proceedings of the 20th International Workshop on Mobile Computing Systems and Applications, HotMobile 2019, Santa Cruz, CA, USA, February 27-28, 2019*, Alec Wolman and Lin Zhong (Eds.). ACM, 153–158. <https://doi.org/10.1145/3301293.3302355>
- [34] Ankit Toshniwal, Siddharth Taneja, Amit Shukla, Karthikeyan Ramasamy, Jignesh M. Patel, Sanjeev Kulkarni, Jason Jackson, Krishna Gade, Maosong Fu, Jake Donham, Nikunj Bhagat, Sailesh Mittal, and Dmitriy V. Ryaboy. 2014. Storm@twitter. In *International Conference on Management of Data, SIGMOD 2014, Snowbird, UT, USA, June 22-27, 2014*, Curtis E. Dyreson, Feifei Li, and M. Tamer Özsu (Eds.). ACM, 147–156. <https://doi.org/10.1145/2588555.2595641>
- [35] TPC-DS [n.d.]. TPC-DS <http://www.tpc.org/tpcds/>.
- [36] UpgradeFlinkApplications [n.d.]. Upgrading Applications and Flink Versions, <https://nightlies.apache.org/flink/flink-docs-release-1.14/docs/ops/upgrading/>.

- [37] Gerhard Weikum and Gottfried Vossen. 2002. *Transactional Information Systems: Theory, Algorithms, and the Practice of Concurrency Control and Recovery*. Morgan Kaufmann.
- [38] Bénard Wiese and Christian Omlin. 2009. Credit card transactions, fraud detection, and machine learning: Modelling time with LSTM recurrent neural networks. In *Innovations in neural information paradigms and applications*. Springer, 231–268.
- [39] Matei Zaharia, Tathagata Das, Haoyuan Li, Timothy Hunter, Scott Shenker, and Ion Stoica. 2013. Discretized streams: fault-tolerant streaming computation at scale. In *ACM SIGOPS 24th Symposium on Operating Systems Principles, SOSP '13, Farmington, PA, USA, November 3–6, 2013*, Michael Kaminsky and Mike Dahlin (Eds.). ACM, 423–438. <https://doi.org/10.1145/2517349.2522737>